Figure S1.

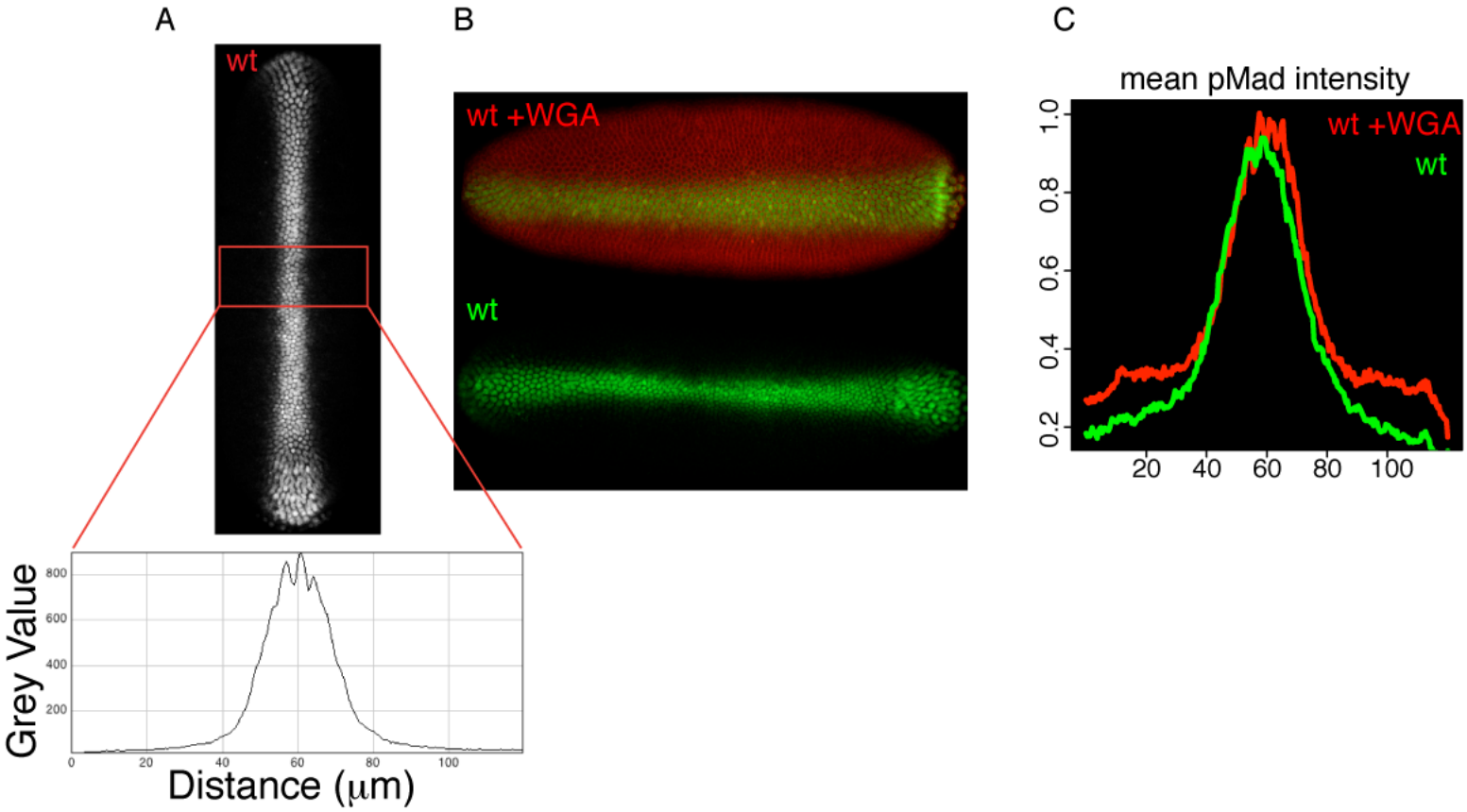
A
wt
B
wt +WGA
wt
C
mean pMad intensity
wt +WGA
wt
1.0
0.8
0.6
0.4
0.2
20
40
60
80
100
Grey Value
800
600
400
200
0
20
40
60
80
100
Distance (μm)

Figure S2.

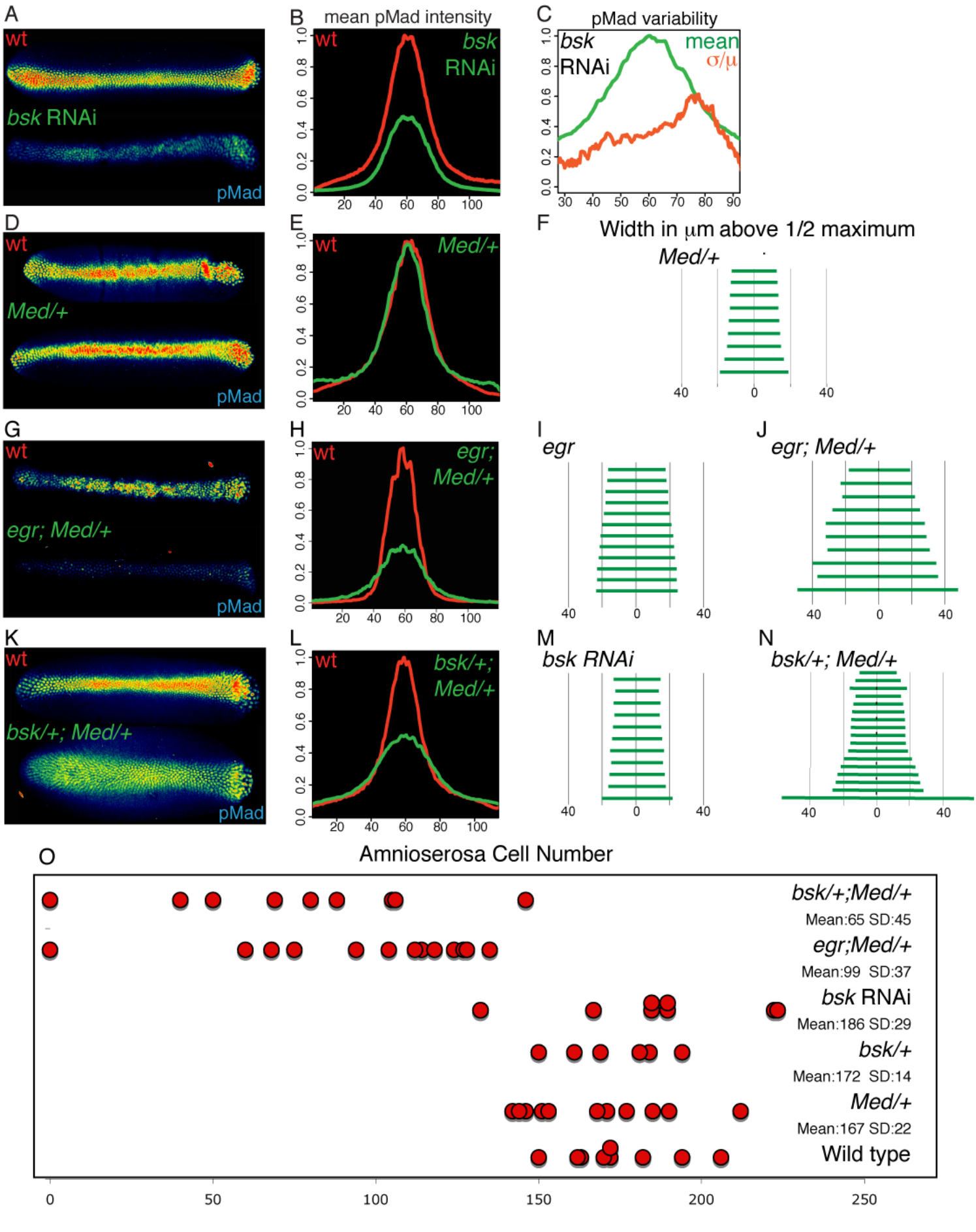
A
wt
bsk RNAi
pMad
B
mean pMad intensity
wt
bsk RNAi
C
pMad variability
bsk RNAi
mean
σ/μ
D
wt
Med/+
pMad
E
wt
Med/+
F
Width in μm above 1/2 maximum
Med/+
G
wt
egr; Med/+
pMad
H
wt
egr; Med/+
I
egr
J
egr; Med/+
K
wt
bsk/+; Med/+
pMad
L
wt
bsk/+; Med/+
M
bsk RNAi
N
bsk/+; Med/+
O
Amnioserosa Cell Number
bsk/+;Med/+
Mean:65 SD:45
egr;Med/+
Mean:99 SD:37
bsk RNAi
Mean:186 SD:29
bsk/+
Mean:172 SD:14
Med/+
Mean:167 SD:22
Wild type

Figure S3.

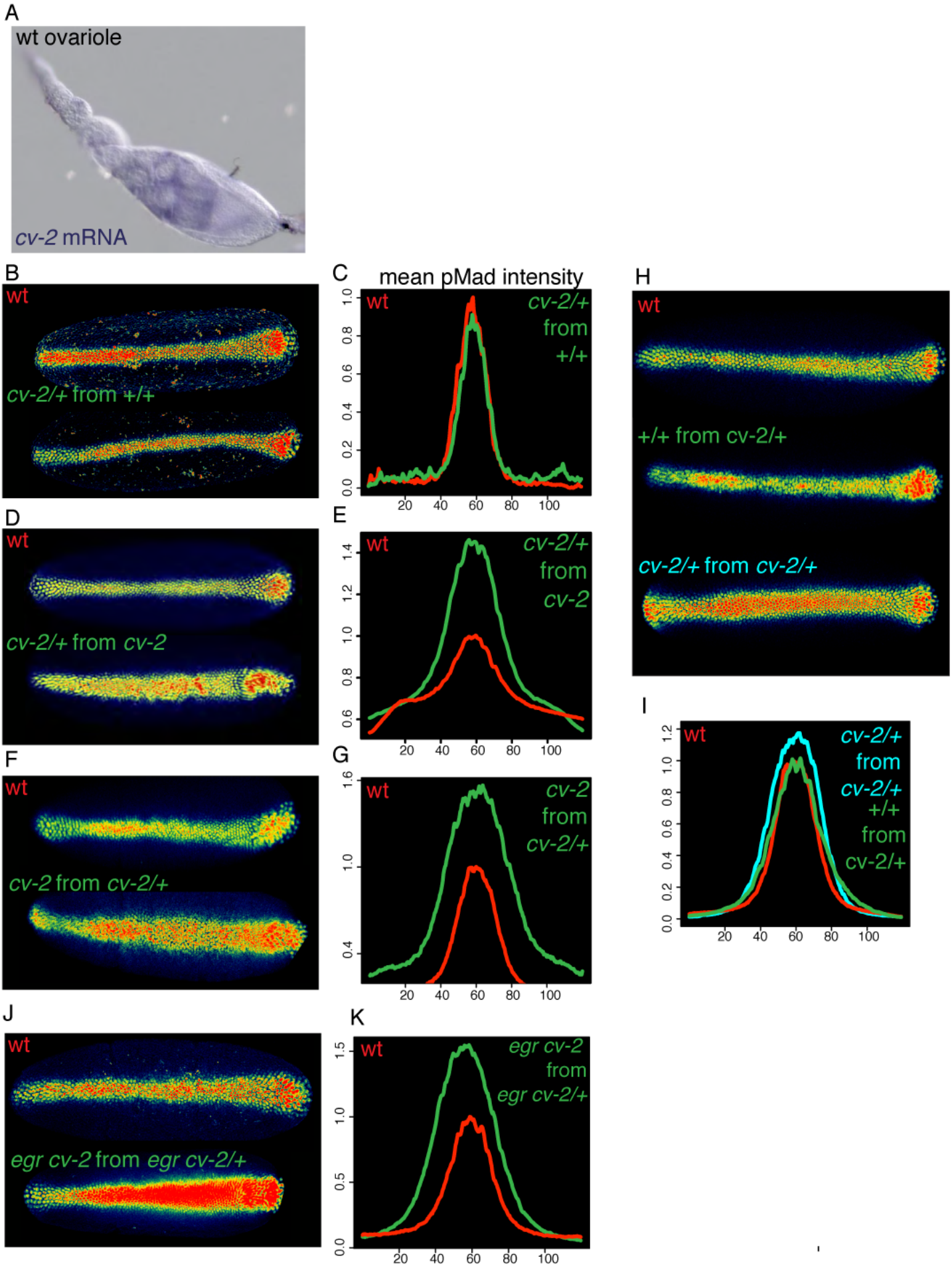
A
wt ovariole
cv-2 mRNA
B
wt
cv-2/+ from +/+
C
mean pMad intensity
wt
cv-2/+ from +/+
D
wt
cv-2/+ from cv-2
E
wt
cv-2/+ from cv-2
F
wt
cv-2 from cv-2/+
G
wt
cv-2 from cv-2/+
H
wt
+/+ from cv-2/+
cv-2/+ from cv-2/+
I
wt
cv-2/+ from cv-2/+
+/+ from cv-2/+
J
wt
egr cv-2 from egr cv-2/+
K
wt
egr cv-2 from egr cv-2/+

FIGURE S4.

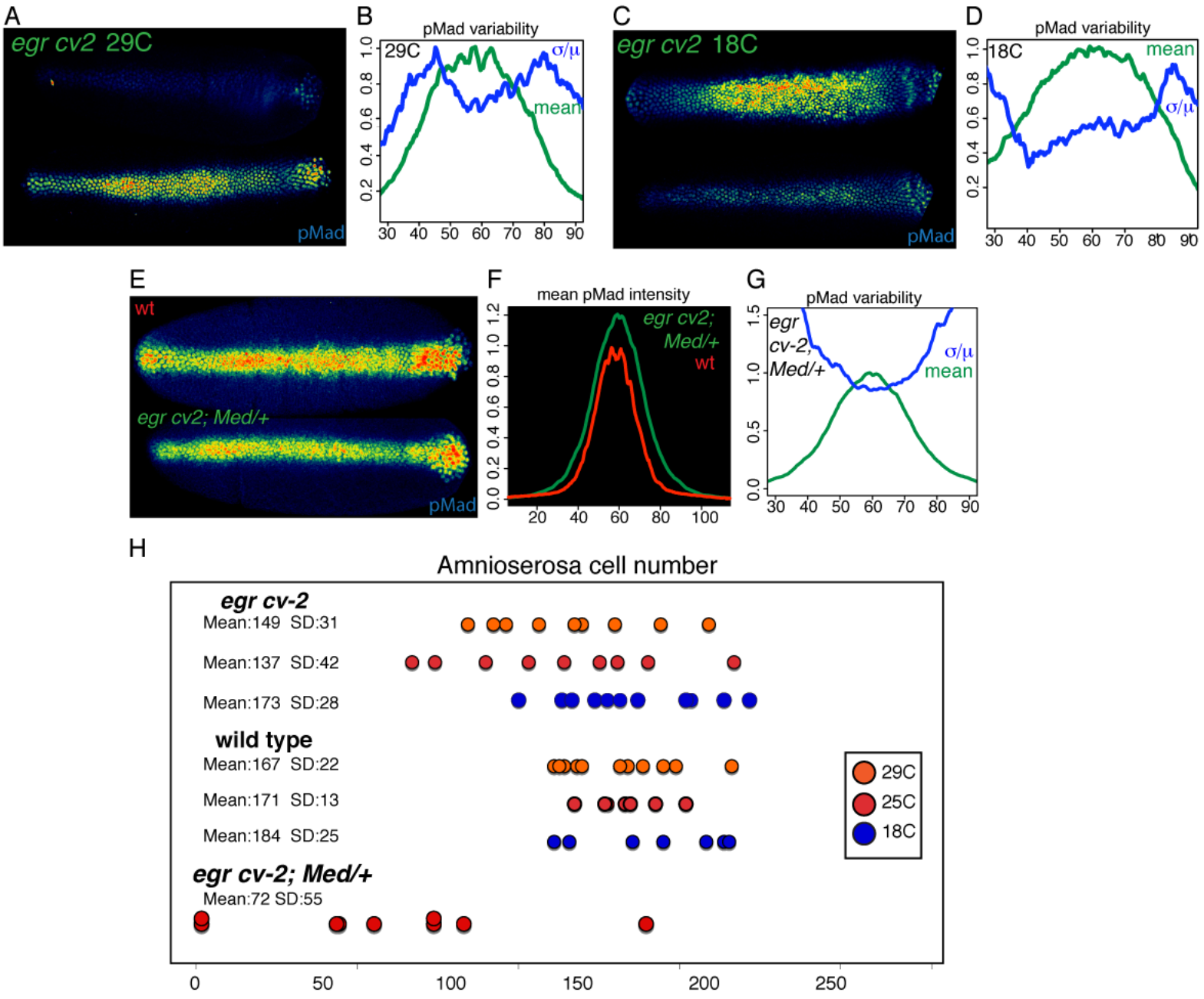
A
egr cv2 29C
pMad
B
pMad variability
29C
σ/μ
mean
C
egr cv2 18C
pMad
D
pMad variability
18C
mean
σ/μ
E
wt
egr cv2; Med/+
pMad
F
mean pMad intensity
egr cv2; Med/+
wt
G
pMad variability
egr cv-2, Med/+
σ/μ
mean
H
Amnioserosa cell number
egr cv-2
Mean:149 SD:31
Mean:137 SD:42
Mean:173 SD:28
wild type
Mean:167 SD:22
Mean:171 SD:13
Mean:184 SD:25
egr cv-2; Med/+
Mean:72 SD:55
29C
25C
18C

Figure S5.

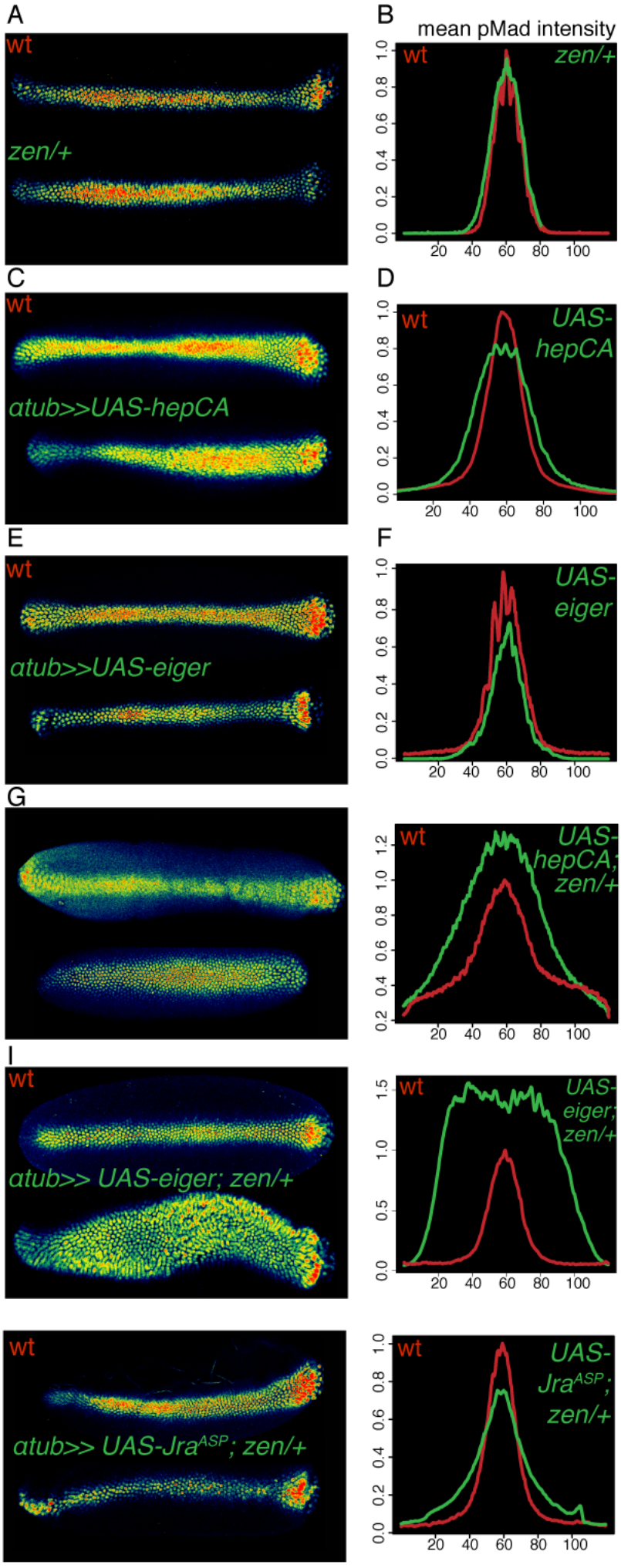
A
wt
zen/+
B
mean pMad intensity
wt
zen/+
C
wt
atub>>UAS-hepCA
D
wt
UAS-hepCA
E
wt
atub>>UAS-eiger
F
UAS-eiger
G
wt
UAS-hepCA; zen/+
I
wt
atub>> UAS-eiger; zen/+
wt
UAS-eiger; zen/+
wt
atub>> UAS-Jra^ASP; zen/+
wt
UAS-Jra^ASP; zen/+

Figure S6.

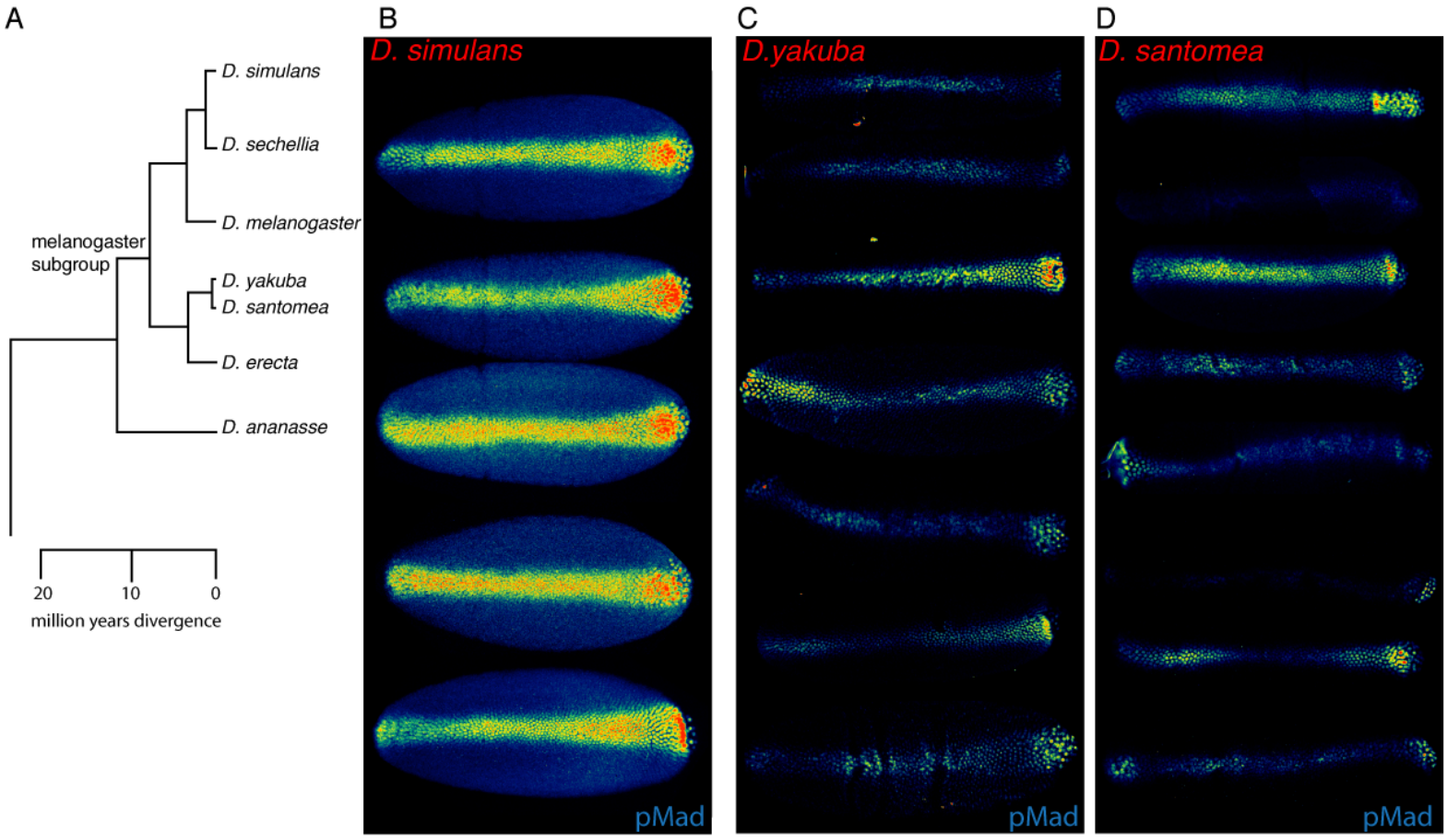
A
B
C
D
D. simulans
D. sechellia
D. melanogaster
D. yakuba
D. santomea
D. erecta
D. ananasse
melanogaster subgroup
20
10
0
million years divergence
D. simulans
D.yakuba
D. santomea
pMad
pMad
pMad

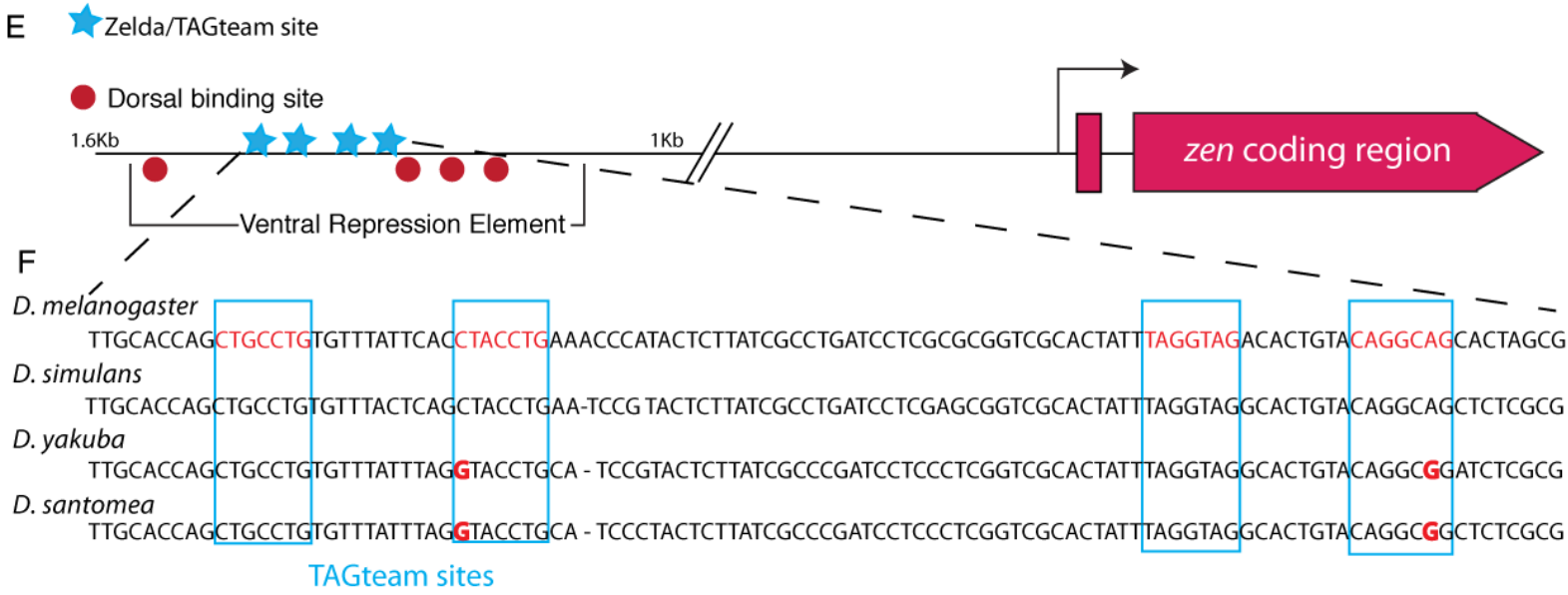
E
Zelda/TAGteam site
Dorsal binding site
1.6Kb
1Kb
zen coding region
Ventral Repression Element
F
D. melanogaster
TTGCACCAGCTGCCTGTGTTTATTCACCTACCTGAAACCCATACTCTTATCGCCTGATCCTCGCGCGGTCGCACTATTTAGGTAGACACTGTACAGGCAGCACTAGCG
D. simulans
TTGCACCAGCTGCCTGTGTTTACTCAGCTACCTGAA-TCCG TACTCTTATCGCCTGATCCTCGAGCGGTCGCACTATTTAGGTAGGCACTGTACAGGCAGCTCTCGCG
D. yakuba
TTGCACCAGCTGCCTGTGTTTATTTAGGTACCTGCA - TCCGTACTCTTATCGCCCGATCCTCCCTCGGTCGCACTATTTAGGTAGGCACTGTACAGGCGGATCTCGCG
D. santomea
TTGCACCAGCTGCCTGTGTTTATTTAGGTACCTGCA - TCCCTACTCTTATCGCCCGATCCTCCCTCGGTCGCACTATTTAGGTAGGCACTGTACAGGCGGCTCTCGCG
TAGteam sites

Supplemental Figure Legends.

Figure S1. Comparative intensity analysis of pMad staining.

(A) For each embryo, a dorsal confocal Z-series of images is first flattened into a SUM projection in ImageJ. A 60 x 120 micron box is centered on the pMad stripe at 50% egg length. For each of the 120 microns along the D/V axis, the average intensity of all AP positions is calculated in Excel and graphed against D/V position in R. (B) Two wild-type embryos, one marked with Alexa633 conjugated wheat germ agglutinin (WGA) dye (top), stained with anti-pMad antibody. (C) The dye has no effect on the pMad intensity as seen in the average of 3 wild-type embryos marked with WGA (red) and 3 without (green).

Figure S2. Enhancement of the *egr*/JNK phenotype by maternal heterozygosity for the null *Med*^{13} allele.

(A-C) Elimination of maternal *bsk* activity is similar to loss of *egr* activity. Representative pMad staining (A), average intensities (B) and variability (C) of 6 wild-type and 6 *bsk* RNAi embryos. (D-F) Maternal heterozygosity for the co-Smad *Medea* does not affect pMad staining. Representative pMad staining (D) and average intensities (E) of 6 wild-type embryos and 6 embryos from *Med*^{13}/+ females. (F) Width in microns of the region of individual embryos from *Med*^{13}/+ females where pMad intensity is greater than 50% of peak mean intensity. The half maximal widths are similar to those in wild-type embryos (Figure 1D). (G-J) *egr* embryos from *egr*; *Med*^{13}/+ females have a greater variability in spatial extent of pMad staining than *egr* embryos or embryos from *Med*^{13}/+ females. Representative pMad staining (G) and average intensities (H) of 6 wild-type embryos and 6 *egr* embryos from *egr*; *Med*^{13}*/TM3 hb-lacZ* females. Width in microns of the region of individual *egr* embryos (I) or *egr* embryos from *egr*; *Med*^{13}*/TM3 hb-lacZ* females (J) where pMad intensity is greater than 50% of peak mean intensity. pMad staining in *egr* embryos is significantly expanded from wild type ($t = 8.7142$, $df = 20.263$, p-value = 1.364e-08). (K-N) Embryos from *bsk*/+; *Med*^{13}/+ females have a greater variability in the spatial extent of pMad staining than *bsk* RNAi embryos or embryos from *Med*^{13}/+ females. pMad staining in representative embryos (K) and average intensities (L) of 8 wild-type embryos and 21 embryos from *Df(bsk)/CyO ftz-lacZ*; *Med*^{13}*/TM3 hb-lacZ* females. Width in microns of the region of individual *bsk RNAi* embryos (M) or embryos from *Df(bsk)/CyO ftz-lacZ*; *Med*^{13}*/TM3 hb-lacZ* females (N) where pMad intensity is greater than 50% of peak mean intensity. (O) Amnioserosa cell numbers in wild-type embryos, embryos from *Med*/+ females, embryos with mutations in the *egr*/JNK pathway (*egr* embryos, *bsk* RNAi embryos, and embryos from *bsk*/+ females) or double mutant embryos with both *Med* and JNK pathway mutations. Double mutant embryos had fewer amnioserosa cells and a higher level of variation between embryos than the respective single mutants. All embryos were raised at 25^{o}C.

Figure S3. Maternal and zygotic contributions of *cv-2*.

(A) A wild-type ovariole hybridized with antisense *cv-2* probe, showing expression in the nurse cells of an egg chamber. (B-I) pMad staining in representative embryos (B,D,F,H) and average intensities (C,E,G,I) of 4 wild-type compared to 5 *cv-2*/+ embryos from +/+ females (B,C), 5 wild-type embryos compared to 6 *cv-2*/+ embryos from *cv-2/cv-2* females (D,E), 3 wild-type embryos compared to 9 *cv-2*/*cv-2* embryos from *cv-2*/*CyO ftz-lacZ* females (F,G), and 8 wild-type embryos compared to 8 +/+ embryos and 5 *cv-2*/+ embryos from *cv-2*/*CyO ftz-lacZ* females (H,I). While *cv-2*/+ embryos from +/+ females have a wild-type pMad pattern (C), *cv-2*/+ embryos from *cv-2*/*cv-2* females have a 1.5 fold increase in pMad intensity compared to wild

type (E), indicative of an effect of maternal Cv-2 protein on BMP signaling. While *CyO ftz-lacZ* /+ embryos from *cv-2*/*CyO ftz-lacZ* females have a wild-type pMad pattern (I), *cv-2*/+ embryos from *cv-2*/*CyO ftz-lacZ* females have a 1.2 fold increase in pMad intensity compared to wild type (I), and *cv-2*/*cv-2* embryos from *cv-2/CyO ftz-lacZ* females have a 1.5 fold increase in pMad intensity compared to wild type (G), indicative of the effect of zygotic *cv-2* activity on BMP signaling. (J-K) pMad staining in representative embryos (J) and average intensities (K) of 5 wild-type compared to 10 *egr cv-2* embryos from *egr cv-2*/*CyO ftz-lacZ* females. While *egr cv-2* embryos have an average pMad intensity that is equivalent to wild-type embryos (Figures 3G and 3H), *egr cv-2* embryos from *egr cv-2/CyO ftz-lacZ* females have an average intensity that is 1.5 fold greater than the wild type, indicating that wild-type maternal Cv-2 protein can elevate BMP signaling in the absence of zygotic *cv-2* activity.

Figure S4. Amnioserosa specification in *egr cv-2* embryos is not sensitive to temperature, but is sensitive to genetic perturbation of BMP signaling.
(A-D) *egr cv-2* embryos raised at different temperatures. Representative pMad staining (A,C) and variability (B,D) of 8 *egr cv-2* embryos raised at 29^{o}C (A,B) or 18^{o}C (C,D). (E-G) *egr cv-2* embryos from *egr cv-2*; *Med*/+ females. (E-G) Representative pMad staining (E), mean intensity (F), and variability (G) of 8 wild-type embryos and 12 *egr cv-2* embryos from *egr cv-2*; *Med*/+ females. (H) Amnioserosa cell number in wild-type and *egr cv-2* embryos at different temperatures and in *egr cv-2* embryos from *egr cv-2*; *Med*/+ females.

Figure S5. The pre-gastrula activity of *zen* antagonizes BMP signaling.
(A-J) Uniform expression of *egr* or a constitutively-active form of *hemipterous (HepCA)* by a strong maternal driver (α*tub* Gal4) does not change pMad signaling in otherwise wild-type embryos, but increases pMad signaling in zen^{7}/+ embryos. Representative pMad staining (A,C,E,G,I) and average intensities (B,D,F,H,J) of 5 wild-type and 8 zen^{7}/+embryos (A,B), 6 wild-type and 6 *UAS-HepCA* embryos (C,D), 4 wild-type and 6 *UAS-eiger* embryos (E,F), 5 wild-type and 7 *UAS-HepCA*; *zen*/+ embryos (G,H), 6 wild-type and 6 *UAS-egr*; *zen*/+ embryos (I,J). (K-L) Uniform expression of an activated form *Drosophila* Jun homolog, *Jra* (Jra^{ASP}), does not increase pMad staining in *zen*/+ embryos. Representative pMad staining (K) and average intensities (L) of 6 wild-type and 9 *UAS-*Jra^{ASP}; *zen*/+ embryos.

Figure S6. Phylogeny, Zelda binding sites, and BMP signaling in *D. simulans*, *D. yakuba* and *D. santomea* embryos.
(A) Phylogenetic tree of the *melanogaster* group of *Sophophora*. The last common ancestor between *D. melanogaster* and *D. yakuba* was approximately 12.4 million years ago. Figure adapted from [S1]. (B-D) pMad staining in sets of *D. simulans* (B), *D. yakuba* (C), or *D. santomea* (D) embryos. The embryo to embryo variability in the intensity of staining in the *D. simulans* embryos is very low, with a CV less than 0.25 throughout the signaling domain. (E) A schematic of the cis regulatory elements of the *D. melanogaster zen* promoter, adapted from [S2] and [S3], showing the extent of the ventral repression element (VRE), as defined by transgenic analysis. Dorsal has four binding sites in the VRE (red circles) as defined by DNA binding assays [S4]. The VRE contains a 91 bp region with four TAGteam sites (blue stars). (F) The sequence of the 91 bp region that contains the TAGteam sites from *D. melanogaster*, *D. simulans, D. yakuba*, and *D. santomea*. The sites are boxed in blue and the *D. melanogaster* motifs are highlighted in red. Both the *D. yakuba* and *D. santomea* sequences of the second and

fourth sites contain a single base pair substitution: a C→G change in the first base of the second site, and an A→G change in the second to last base of the last site.

Table S1.

	wt	*UAS-eiger*	*UAS-hepCA*	*zen*/+	*UAS-eiger*; *zen*/+	*UAS-hepCA*; *zen*/+	*UAS-JraASP*; *zen*/+
Mean	171	170	176	165	274	216	155
SD	13	30	32	34	72	97	35

Table S1. Mean and standard deviation of amnioserosa cell number in embryos of the genotypes in Figures S5A–S5L.

Table S2.

	D. yakuba			*D. santomea*		
	18°C	25°C	29°C	18°C	25°C	29°C
Mean	150	129	148	179	183	145
SD	23	15	25	36	37	25

Table S2. Mean and standard deviation of amnioserosa cell number in *D. santomea* and *D. yakuba* embryos raised at 18°, 25° and 29°C.

Supplemental Experimental Procedures.

Image analysis for anti-pMad staining.

Embryos stained with the anti-pMad antibody were imaged as dorsal view Z-stacks using a Zeiss LSM 510 scanning confocal microscope on the 20x objective. For comparative intensity analysis, embryos of both the wild-type control and the experimental genotype were imaged on the same day using identical settings. Embryos at the onset of gastrulation were staged by the initiation of the cephalic furrow, without the appearance of the transverse furrow or initiation of germ band extension. This stage persists for ~10 minutes at 25C. All image analysis was conducted in ImageJ. To quantify the intensity of pMad staining, a 32-bit SUM projection of the Z-stacks was made. The pMad staining intensity of the projection was then measured in a box of 60 microns along the A/P axis by 120 microns along the D/V axis at 50% embryo length, centered on the dorsal midline (Figure S1A). The average intensity of pMad staining for each D/V position was calculated by averaging the intensities of the A/P column at each D/V row. The mean intensity traces for all embryos of that genotype were then averaged together in Excel.

To mark embryos of two different genotypes for comparative intensity analysis, fixed wild-type embryos were first incubated in a 1:1000 solution of Wheat Germ Agglutinin (WGA) conjugated to Alexa633 dye in PBT (Invitrogen). After a minimum of five three minute washes with resuspension in PBT, the marked embryos were transferred to the tube containing fixed embryos of the other genotype and antibody staining proceeded as described, beginning with blocking. Control experiments (Figures S1B and S1C) showed that there is no quantifiable difference in pMad staining between wild-type *D. melanogaster* embryos marked with WGA compared to unmarked wild-type embryos.

The mean intensities of experimental genotypes were normalized to the peak wild-type mean intensity of their imaging set. To combine multiple independent collections of images, the intensities of the experimental genotype embryos in each collection were first normalized to their respective wild-type control and then averaged together. The variability in pMad intensity (σ/μ) in the population of embryos of the same genotype was calculated by dividing the standard deviation (σ) of intensities by the mean (μ) intensity for a given D/V position in the collection of embryos. To map variability to regions of the pMad domain, σ/μ values were then plotted against the self-normalized mean intensity of the genotype. All traces were plotted in R. Mean intensity values generally represent a minimum of 6 embryos per genotype.

For image presentation, representative SUM projections of individual embryos were converted to 8 bit. The average peak intensity of the wild-type control image was then used to scale both the wild-type and experimental embryo intensity using Photoshop. The peak mean intensity value of the wild-type image was set to a white value of 200 using the Curves function, with non-linear transformation, and the identical scaling was applied to the experimental image. A colored heat map of intensity was then applied to the scaled images in ImageJ.

Embryos homozygous for a lethal mutation were derived from heterozygous females that carried that mutation in *trans* to a balancer carrying an early embryonic *lacZ* reporter: *CyO, ftz-lacZ* or *TM3, hb-lacZ*. Embryos of the genotype of interest were identified by the absence of staining by the anti β-galactosidase antibody.

For crosses in which pMad staining was assayed in embryos from a heterozygous maternal genotype, the mutations in the parental females were in *trans* to balancers marked with a *lacZ* reporter gene expressed in the early embryo. Such experiments included embryos derived from *Df(bsk)/CyO, ftz-lacZ* or Med^{13}*/TM3, hb-lacZ* females mated with wild-type males. Although control experiments for each cross indicated that the zygotic genotype did not influence pMad

staining (not shown), the zygotic genotypes were standardized by assaying only embryos lacking anti β-galactosidase staining.

Amnioserosa quantification.

The number of amnioserosa cells was quantified in *D. melanogaster* embryos by staining with a mouse monoclonal anti-Hindsight antibody, IG9. Amnioserosa quantification in *D. yakuba* and *D. santomea* embryos used a polyclonal rabbit anti-Dorsocross 2 serum. Both antibodies heavily stain the nuclei of amnioserosa cells, which are distinguished by their large size and high intensity of staining. Stage 10-13 embryos from each species were stained and were imaged using confocal microscopy. A projection of the Z-stack of images for each side of the embryo was made and the individual nuclei counted manually in ImageJ using the Cell Counter plug-in.

Statistical methods and comparisons of number and variance in amnioserosa specification and peak pMad staining.

All tests were conducted in R [R Development Core Team (2010). R: A language and environment for statistical computing. R Foundation for Statistical Computing, Vienna, Austria. http://www.R-project.org].

Number of amnioserosa cells specified.

The number of amnioserosa cells in *bskRNAi* embryos was not significantly different from the wild type, while the number of amnioserosa cells in *egr* was different from wild type (Student's t-test, p=0.26 and p=0.045 respectively).

Variability in amnioserosa specification

All distributions were first assayed for normality by the Shapiro-Wilk test. The amnioserosa count distributions from all genotypes and species were normal.

The variability in amnioserosa specification between wild-type, *egr* and *cv-2* embryos is not significantly different. The F-Test values for equality of variance are:

egr and wild type

F = 0.75, num df = 7, denom df = 6, p-value = 0.709

cv-2 and wild type

F = 0.4047, num df = 7, denom df = 10, p-value = 0.2425

The variability in amnioserosa specification in *egr cv-2* embryos is unequal to either *egr* or *cv-2* single mutants or to the wild type. The F-Test values for equality of variance are:

egr and *egr cv-2*

F = 0.0847, num df = 6, denom df = 9, p-value = 0.007091

cv-2 and *egr cv-2*

F = 0.1569, num df = 10, denom df = 9, p-value = 0.007784

wild type and *egr cv-2*

F = 0.0635, num df = 7, denom df = 9, p-value = 0.001479

The variability in amnioserosa specification in *D. melanogaster* embryos is unequal to that in *D. santomea* embryos, but is similar to that in *D. yakuba* embryos. The F-Test values for equality of variance are:

D. melanogaster and *D. santomea*

F = 0.1319, num df = 7, denom df = 10, p-value = 0.01346.

D. melanogaster and *D. yakuba*
F = 0.3484, num df = 7, denom df = 9, p-value = 0.1784.

Peak pMad staining

To compare the distributions of pMad intensities between populations of embryos of two genotypes, we first determined the normalized average peak pMad intensity for each embryo, independent of position of the peak on the D/V axis. Then, because the distribution of peak pMad intensity in both the *egr cv-2* and the *D. santomea* embryo populations failed the Shapiro-Wilk test of normality, the statistical comparison of variability of peak pMad intensity between genotypes was the non-parametric ANOVA, Kruskal-Wallis test. *D. yakuba* and *zen* mutant embryos had a normal distribution of pMad intensities, thus the Bartlett test for homogeneity of variance was used.

Each single mutant has peak pMad intensity variability indistinguishable from wild type. Conversely, the peak pMad intensity in *egr cv-2* double mutant embryos is unequal to that in wild type.

egr and wild type
Kruskal-Wallis chi-squared = 1.127, df = 1, p-value = 0.2884.
cv-2 and wild type
Kruskal-Wallis chi-squared = 0.5933, df = 1, p-value = 0.4411.
egr cv-2 and wild type
Kruskal-Wallis chi-squared = 6.2208, df = 1, p-value = 0.01263.

The variability of peak pMad intensity is unequal between *D. melanogaster* embyos and *D. santomea* embryos. *D. melanogaster* and *D. yakuba* embryos are not significantly different at an alpha level of 0.05, however this may be reflective of the *D. yakuba* population's flanks registering the maximal σ/μ values. However, the variance of *D. yakuba* peak intensity is significantly greater than *D. melanogaster,* as indicated by the One-sided F-Test. There is equal variability of peak pMad intensity between *zen* mutant embryos and *D. yakuba* embryos.

D. melanogaster and *D. santomea*
Kruskal-Wallis chi-squared = 10.1712, df = 1, p-value = 0.001426
D. melanogaster and *D. yakuba*
Bartlett's K-squared = 3.6118, df = 1, p-value = 0.05737
D. melanogaster and *D. yakuba*
One-sided F-Test = F = 3.9437, num df = 11, denom df = 8, p-value = 0.03088
zen and *D. yakuba*
Bartlett's K-squared = 0.1079, df = 1, p-value = 0.7425

Embryo collections.

All fly stocks were maintained at 18-29ºC, as indicated, on standard cornmeal molasses medium. Embryos were collected from depositions on agar apple juice plates. For staging at the onset of gastrulation, collections at 25ºC were from cups of flies allowed to deposit eggs for an hour. After 2 hours and 45 minutes the eggs were dechorionated in bleach and fixed for 18 minutes in 3.7% Formaldehyde PEM and Heptane. For 18ºC collections, flies were allowed to deposit eggs for one hour and embryos were incubated for 3 hours 30 minutes prior to fixation. For 29ºC collections, flies were allowed to deposit eggs for one hour, and embryos were fixed after 2 hours 20 minutes.

Fly stocks.

The following stocks were obtained from the Bloomington stock center:

2061 *dpp^{H46} wg^{Sp-1} cn^{1} bw^{1}/CyO, P{w[+mC]=dpp-P23}RP1*

2260 *zen^{7} red^{1} e^{1}/TM3, Sb^{1} Ser^{1}*

4937 *w^{1118}; P{w[+mC]=GAL4::VP16-nos.UTR}CG6325[MVD1]*

7340 *ru^{1} h^{1} P{ry[+t7.2]=neoFRT}82B sr^{1} e^{s} Med^{13}/TM3, Sb^{1}, hb-lacZ*

The following stocks were obtained from the VDRC stock center:

v34138 *bsk* RNAi

The following stocks were gifts from the fly community: *D. yakuba* and *D. santomea* synthetic lines and *D. santomea* isofemale line 2 were gifts from Dr. D. Matute [S5]. *cv-2^{KO2}* was a gift from Dr. M. O'Connor [S6]. *eiger^{3}* and UAS-*eiger* were gifts from Dr. M. Miura [S7]. The JNK pathway mutations have been described previously: *Df(2L)flp147E* [S8], UAS-*HepCA* [S9], and UAS-*Jun^{Asp}* [S10].

Antibody staining.

Embryo collection and fixation was done using standard techniques [S11]. The rabbit anti-pMad antibody, made by D. Vasiliauskas and S. Morton, was a gift from Drs. E. Laufer and T. Jessell and was used at 1:2000. The mouse monoclonal anti-Hindsight antibody, IG9 (Developmental Studies Hybridoma Bank), was used at 1:10. The rabbit anti-Dorsocross-2 antibody, a gift from Dr. M. Frasch [S12], was pre-absorbed, then used at 1:500. The rabbit anti-Eiger antibody, a gift from Dr. M. Muira [S13], was used at 1:500. The mouse anti-β galactosidase antibody (Promega Z3781) was used at 1:1000, as was the rabbit anti-GFP (AbCam ab6556) antibody. All secondary antibodies were used at 1:1000 and were purchased from Jackson Laboratories.

In situ hybridization.

For in situ hybridization analysis, anti-sense RNA probes were synthesized using DIG labeled dNTPs and Roche T3 or T7 polymerase kits. Hybridization was followed by incubation with Roche anti-DIG Fab fragments conjugated to alkaline phosphotase and detection of the RNA probes used the Roche NBT/BCIP reaction kit. All embryos were mounted in 95% glycerol prior to imaging.

The *D. yakuba zen* probe was synthesized from a genomic DNA preparation using the following primers:

Forward ACGAACCGCCTTTACCAGTGTC,

Reverse CCAGGATTGAGTAGCCAGGATG.

A 600 bp fragment was then cloned into pGEM from Promega. The same probe was used to detect *zen* transcription in *D. santomea* embryos.

Generation of *Medea* null germline clones.

To generate the *Medea^{13}* germline clones, *ru^{1} h^{1} P{ry[+t7.2]=neoFRT}82B sr^{1} e^{s} Med^{13}/TM3, Sb^{1}, hb-lacZ* females were crossed to *hs>FLP*/Y; *P{ry[+t7.2]=neoFRT}82B P{w[+mC]=ovoD1-18}3R*/TM3 *Sb^{1}* males in bottles and allowed to lay eggs for 2 days. After two days the crosses were flipped into new bottles. When wandering larvae appeared in these bottles, or after ~5 days at 25ºC, the bottles were subjected to daily 2 hour heat-shock at 37ºC

until adults eclosed. Non-TM3 females were collected and mated to *ru^{1} h^{1} P{ry[+t7.2]=neoFRT}82B sr^{1} e^{s} Med^{13}/TM3, Sb^{1}, hb-lacZ* males. Embryos derived from this cross were collected and stained with both anti-pMad and anti-β-galatosidase antibodies. Only those embryos entirely null for *Medea*, without β-galatosidase staining, were used in this analysis.

Supplemental References.

S1. Lachaise, D., Cariou, M.L., David, J.R., Lemeunier, F., Tsacas, L., Ashburner, M. (1988). Historical biogeography of the *Drosophila* melanogaster species subgroup. . Evolutionary Biology *22*, 159--225.

S2. Markstein, M., Markstein, P., Markstein, V., and Levine, M.S. (2002). Genome-wide analysis of clustered Dorsal binding sites identifies putative target genes in the *Drosophila* embryo. Proc. Natl. Acad. Sci. U S A *99*, 763-768.

S3. Liang, H.L., Nien, C.Y., Liu, H.Y., Metzstein, M.M., Kirov, N., and Rushlow, C. (2008). The zinc-finger protein Zelda is a key activator of the early zygotic genome in *Drosophila*. Nature *456*, 400-403.

S4. Ip, Y.T., Kraut, R., Levine, M., and Rushlow, C.A. (1991). The dorsal morphogen is a sequence-specific DNA-binding protein that interacts with a long-range repression element in *Drosophila*. Cell *64*, 439-446.

S5. Matute, D.R., Novak, C.J., and Coyne, J.A. (2009). Temperature-based extrinsic reproductive isolation in two species of *Drosophila*. Evolution *63*, 595-612.

S6. Serpe, M., Umulis, D., Ralston, A., Chen, J., Olson, D.J., Avanesov, A., Othmer, H., O'Connor, M.B., and Blair, S.S. (2008). The BMP-binding protein Crossveinless 2 is a short-range, concentration-dependent, biphasic modulator of BMP signaling in *Drosophila*. Dev. Cell. *14*, 940-953.

S7. Igaki, T., Kanda, H., Yamamoto-Goto, Y., Kanuka, H., Kuranaga, E., Aigaki, T., and Miura, M. (2002). Eiger, a TNF superfamily ligand that triggers the *Drosophila* JNK pathway. EMBO J *21*, 3009-3018.

S8. Riesgo-Escovar, J.R., Jenni, M., Fritz, A., and Hafen, E. (1996). The *Drosophila* Jun-N-terminal kinase is required for cell morphogenesis but not for DJun-dependent cell fate specification in the eye. Genes Dev. *10*, 2759-2768.

S9. Weber, U., Paricio, N., and Mlodzik, M. (2000). Jun mediates Frizzled-induced R3/R4 cell fate distinction and planar polarity determination in the *Drosophila* eye. Development *127*, 3619-3629.

S10. Treier, M., Bohmann, D., and Mlodzik, M. (1995). JUN cooperates with the ETS domain protein pointed to induce photoreceptor R7 fate in the *Drosophila* eye. Cell *83*, 753-760.

S11. Patel, N.H. (1994). Imaging neuronal subsets and other cell types in whole-mount *Drosophila* embryos and larvae using antibody probes. In *Drosophila melanogaster:* Practical Uses in Cell and Molecular Biology, L.S.B. Goldstein, Fyrburg, E., ed. (San Diego, CA: Academic Press, Inc.), pp. 446-485.

S12. Reim, I., Lee, H.H., and Frasch, M. (2003). The T-box-encoding Dorsocross genes function in amnioserosa development and the patterning of the dorsolateral germ band downstream of Dpp. Development *130*, 3187-3204.

S13. Igaki, T. (2009). Correcting developmental errors by apoptosis: lessons from *Drosophila* JNK signaling. Apoptosis *14*, 1021-1028.